NASA/TM–2011-217316

Deployment of a Pressure Sensitive Paint System for Measuring Global Surface Pressures on Rotorcraft Blades in Simulated Forward Flight

Preliminary PSP Results from Test 581 in the 14- x 22-Foot Subsonic Tunnel

Anthony Neal Watkins, Bradley D. Leighty, and William E. Lipford
Langley Research Center, Hampton, Virginia

Oliver D. Wong
U.S. Army Aeroflightdynamics Directorate, Joint Programs Office, Hampton, Virginia

Kyle Z. Goodman
ATK, Hampton, Virginia

James Crafton, Alan Forlines, and Larry Goss
Innovative Scientific Solutions, Inc., Dayton, Ohio

James W. Gregory and Thomas J. Juliano
Ohio State University, Columbus, Ohio

December 2011

NASA STI Program . . . in Profile

Since its founding, NASA has been dedicated to the advancement of aeronautics and space science. The NASA scientific and technical information (STI) program plays a key part in helping NASA maintain this important role.

The NASA STI program operates under the auspices of the Agency Chief Information Officer. It collects, organizes, provides for archiving, and disseminates NASA's STI. The NASA STI program provides access to the NASA Aeronautics and Space Database and its public interface, the NASA Technical Report Server, thus providing one of the largest collections of aeronautical and space science STI in the world. Results are published in both non-NASA channels and by NASA in the NASA STI Report Series, which includes the following report types:

- TECHNICAL PUBLICATION. Reports of completed research or a major significant phase of research that present the results of NASA programs and include extensive data or theoretical analysis. Includes compilations of significant scientific and technical data and information deemed to be of continuing reference value. NASA counterpart of peer-reviewed formal professional papers, but having less stringent limitations on manuscript length and extent of graphic presentations.

- TECHNICAL MEMORANDUM. Scientific and technical findings that are preliminary or of specialized interest, e.g., quick release reports, working papers, and bibliographies that contain minimal annotation. Does not contain extensive analysis.

- CONTRACTOR REPORT. Scientific and technical findings by NASA-sponsored contractors and grantees.

- CONFERENCE PUBLICATION. Collected papers from scientific and technical conferences, symposia, seminars, or other meetings sponsored or co-sponsored by NASA.

- SPECIAL PUBLICATION. Scientific, technical, or historical information from NASA programs, projects, and missions, often concerned with subjects having substantial public interest.

- TECHNICAL TRANSLATION. English-language translations of foreign scientific and technical material pertinent to NASA's mission.

Specialized services also include creating custom thesauri, building customized databases, and organizing and publishing research results.

For more information about the NASA STI program, see the following:

- Access the NASA STI program home page at *http://www.sti.nasa.gov*

- E-mail your question via the Internet to help@sti.nasa.gov

- Fax your question to the NASA STI Help Desk at 443-757-5803

- Phone the NASA STI Help Desk at 443-757-5802

- Write to:
  NASA STI Help Desk
  NASA Center for AeroSpace Information
  7115 Standard Drive
  Hanover, MD 21076-1320

NASA/TM–2011-217316

Deployment of a Pressure Sensitive Paint System for Measuring Global Surface Pressures on Rotorcraft Blades in Simulated Forward Flight

Preliminary PSP Results from Test 581 in the 14- x 22-Foot Subsonic Tunnel

Anthony Neal Watkins, Bradley D. Leighty, and William E. Lipford
Langley Research Center, Hampton, Virginia

Oliver D. Wong
U.S. Army Aeroflightdynamics Directorate, Joint Programs Office, Hampton, Virginia

Kyle Z. Goodman
ATK, Hampton, Virginia

James Crafton, Alan Forlines, and Larry Goss
Innovative Scientific Solutions, Inc., Dayton, Ohio

James W. Gregory and Thomas J. Juliano
Ohio State University, Columbus, Ohio

National Aeronautics and
Space Administration

Langley Research Center
Hampton, Virginia 23681-2199

December 2011

Acknowledgments

The authors would like to thank the staff from the 14- x 22-foot Subsonic Tunnel for their efforts in making this test possible. Funding for this test was provided by the Subsonic Rotary Wing project under the Fundamental Aeronautics Program.

Available from:

NASA Center for AeroSpace Information
7115 Standard Drive
Hanover, MD 21076-1320
443-757-5802

Abstract

This report will present details of a Pressure Sensitive Paint (PSP) system for measuring global surface pressures on the tips of rotorcraft blades in simulated forward flight at the 14- x 22-Foot Subsonic Tunnel. The system was designed to use a pulsed laser as an excitation source and PSP data was collected using the lifetime-based approach. With the higher intensity of the laser, this allowed PSP images to be acquired during a single laser pulse, resulting in the collection of crisp images that can be used to determine blade pressure at a specific instant in time. This is extremely important in rotorcraft applications as the blades experience dramatically different flow fields depending on their position in the rotor disk. Testing of the system was performed using the U.S. Army General Rotor Model System equipped with four identical blades. Two of the blades were instrumented with pressure transducers to allow for comparison of the results obtained from the PSP. This report will also detail possible improvements to the system.

I. Introduction

The accurate determination of spatially continuous pressure and temperature distributions on aerodynamic surfaces is critical for the understanding of complex flow mechanisms and for comparison with computational fluid dynamics (CFD) predictions. Conventional pressure measurements are based on pressure taps and electronically scanned pressure transducers or embedded pressure transducers. While these approaches provide accurate pressure information, pressure taps/transducers are limited to providing data at discrete points. Moreover, the integration of a sufficient number of pressure taps/transducers on a surface can be time and labor intensive and expensive.

This is especially true in rotorcraft research, where the examination of pressure distributions on the blade is vital to advance analytical prediction methods for rotorcraft aerodynamics, acoustics, and interactional effects. There has been considerable research involving pressure measurements on rotor blades.[1-4] However, these measurements typically lack the spatial resolution necessary to capture phenomena such as the nascent tip vortex or dynamic stall. Instrumenting the blades with additional transducers to increase spatial resolution can quickly become prohibitive due to the cost and practicality of fitting a large number of sensors into a small area. In addition, the added centrifugal loads of the pressure transducers can rapidly become unmanageable.

Applying pressure sensitive paint (PSP) to the surface may enable high spatial resolution surface measurements on helicopter rotor blades, thus allowing more accurate analytical prediction methods to be developed. The PSP technique[5-9] exploits the oxygen (O_2) sensitivity of luminescent probe molecules suspended in gas-permeable binder materials. If the test surface under study is immersed in an atmosphere containing O_2 (e.g. air), the recovered luminescence intensity can be described by the Stern-Volmer relationship[10]

$$\frac{I_0}{I} = 1 + K_{SV}(T)P_{O_2} \tag{1}$$

where I_0 is the luminescence intensity in the absence of O_2 (i.e. vacuum), I is the luminescence intensity at some partial pressure of oxygen P_{O2}, and K_{SV} is the Stern-Volmer constant.

Since it is a practical impossibility to measure I_0 in a wind tunnel application, a modified form of the Stern-Volmer equation is typically used. This form replaces the vacuum calibration (I_0) with a reference standard

$$\frac{I_{REF}}{I} = A(T) + B(T)\frac{P}{P_{REF}} \tag{2}$$

where I_{REF} is the recovered luminescence intensity at a reference pressure, P_{REF}. The coefficients A(T) and B(T) are temperature dependent constants for a given PSP formulation and are usually determined beforehand using laboratory calibration procedures.

There are two methods for acquiring PSP data. The most common method used for data acquisition is an "intensity-based" technique. During intensity-based PSP experiments, I_{REF} is typically acquired while the wind tunnel is off or at very low speed and P_{REF} is the static pressure when no wind is applied. Thus I_{REF} is referred to as the "wind-off" intensity. I is the recovered luminescence intensity at some pressure P. Since this data is collected at a specific condition in the wind tunnel, I is also referred to as the "wind-on" intensity. A(T) and B(T) are temperature dependent constants for a given PSP formulation and are usually determined beforehand using laboratory calibration procedures.

A second method of PSP data acquisition is known as "lifetime-based" PSP.[11-15] In the lifetime-based technique, excitation of the PSP is accomplished using a modulated light source (e.g. laser, flash lamp, or pulsed LED arrays). A fast framing camera (intensified CCD or interline transfer CCD) is used to collect the excited state luminescence decay. Typically the decay is approximated by acquiring two or more images at different delay times during and/or after the pulsed excitation and integrating photons for fixed periods of time (i.e. gate widths) that have been predetermined to maximize the pressure sensitivity, as demonstrated in Fig. 1. The first image (Gate 1) usually consists of a short gate width and is collected either during the excitation pulse or shortly after it ends. This can be thought of as the reference image because the excited-state decay has the least pressure sensitivity. The second image (Gate 2) is taken at a later time after the excitation pulse and usually has a longer gate width, ensuring maximum pressure (and temperature) sensitivity. More information on the lifetime technique used in this work can be found in Watkins *et al.*[15]

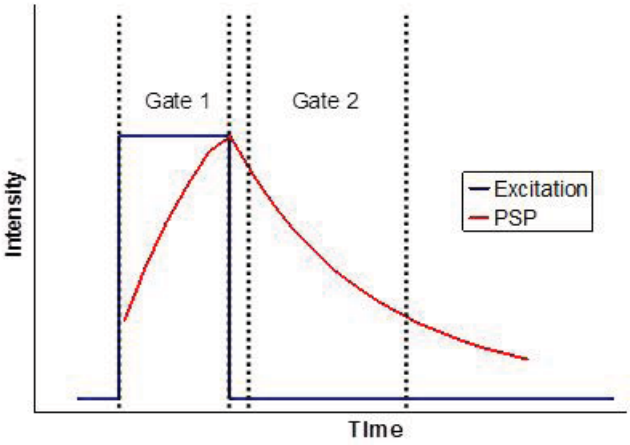

Figure 1. Schematic representation of lifetime-based data acquisition showing excitation (blue) and measured emission (red). The gate regions represent example Gate 1 (during excitation) and Gate 2 (after excitation).

Over the last several years, the U.S. Army Aeroflightdynamics Directorate, Joint Research Program Office, and the NASA Subsonic Rotary Wing Project have partnered to develop the PSP measurement technique for use on rotor blades. This work included an initial proof of concept work in 2003[16] which resulted in the development of instrumented pressure blades for more extended testing in 2008.[17] From these results, a new PSP system based on the previously described system was developed with several modifications for use with rotating test articles. This report will detail these modifications as well as present some preliminary data from the deployment of this system in the 14- x 22-Foot Subsonic Tunnel (hereby abbreviated 14x22) in 2011.

II. Experimental

A. Paint Formulation and Calibration

The two blades that were painted with PSP were coated with a porous polymer formulation that has been described previously.[18-19] This binder can routinely measure dynamic pressure fluctuations at 5 kHz and has been demonstrated to potentially measure fluctuations up to 20 kHz (depending on a variety of factors, including thickness and luminophore). A more detailed review of this formulation and other PSP formulations capable of operating at elevated frequencies can be found in Gregory *et al.*[20] The oxygen sensitive luminophore chosen was platinum meso-tetrakis(pentafluorophenyl) porphine (abbreviated

Pt(TfPP)), which is a common luminophore for PSP applications. A typical application of the PSP involved initially applying the porous polymer binder to a basecoat (usually white to maximize intensity collection efficiency) using conventional spraying techniques. After the binder dries, a solution of the luminophore is then typically over-sprayed onto the binder. This helps to ensure that the luminophore is resting on the surface for maximum interaction with oxygen (thus increasing the frequency response). The disadvantage of this is that the luminophore can degrade fairly quickly. However, this can be alleviated by simply over-spraying with additional luminophore solution. For this work, it was found that over-spraying once a day before running was sufficient for data acquisition.

Calibration of the paint formulation was performed separate from the wind tunnel in a laboratory calibration chamber. This chamber is only capable of measuring pressure and temperature sensitivities; no attempt to determine the frequency response of this paint was attempted. However, as mentioned above, previous testing has shown that this formulation can respond to 5 kHz, well above the frequency range needed for this test. For calibrations, the PSP was applied to 3-inch diameter aluminum coupons that were then placed in the calibration chamber. Illumination of the PSP and acquisition of the luminescent intensity was accomplished using the same system as used in the tunnel.

The PSP formulation was calibrated over a pressure range of 6 to 14.7 psia (41 to 101 kPa) at temperature ranging from 77 to 140 ^{o}F (25 to 60 ^{o}C). A calibration model for the coating was derived by solving Eq. (2) for normalized pressure in terms of the normalized temperature and the gate intensities acquired form the images as described in the previous section. The calibration data showed a multi-dimensional dependence on both pressure and temperature, which can be attributed to the complex nature of oxygen diffusion into the paint binder.[7-9] A linear least squares algorithm was used to fit the data to a modified and expanded version of Eq. (2) above assuming a second order relationship in both temperature and pressure

$$\begin{aligned}(P/P_{REF}) = (a_{11} + a_{12}(T/T_{REF}) + a_{13}(T/T_{REF})^2) + \\ (a_{21} + a_{22}(T/T_{REF}) + a_{23}(T/T_{REF})^2)(G_1/G_2) + \\ (a_{31} + a_{32}(T/T_{REF}) + a_{33}(T/T_{REF})^2)(G_1/G_2)^2\end{aligned} \quad (3)$$

where P and P_{REF} are the pressures, T and T_{REF} are the temperatures, G_1 and G_2 are the intensities in the respective gates (analogous to I_{REF} [G1] and I [G2]), and a_{xy} are the calibration coefficients. A typical calibration is shown in Figure 2.

B. Model and Facilities

The rotor blades that were tested have been constructed from carbon fiber, fiberglass, and aromatic nylon fiber honeycomb trailing-edge core. Each blade has been painted with a white basecoat to enhance the PSP luminescent output (by reflecting the luminescence away from the surface and to the camera) as well as to seal the blade to protect the blade structure from the solvents used in the painting process. The blades are constant chord with a swept-tapered tip and a 14 degree linear twist distribution, using the RC family of airfoils.[21-22] The upper portion of Figure 3 shows the distribution of airfoils and the dimensions of the blades (in inches). Of the

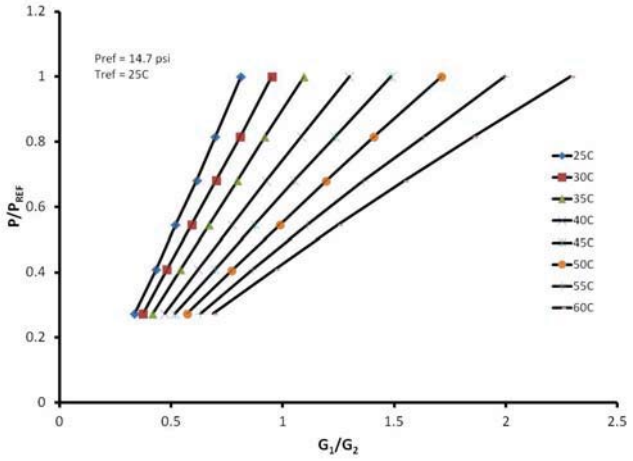

Figure 2. Calibration of PSP formulation for various temperatures and pressures.

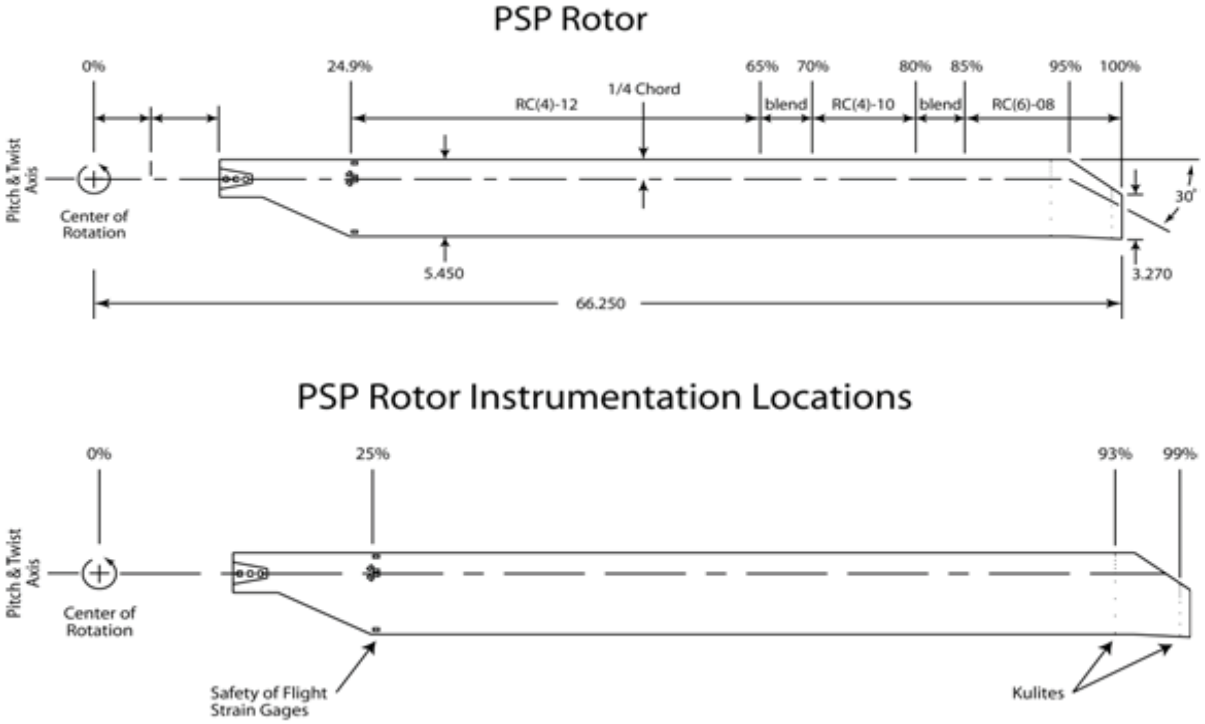

Figure 3. Rotor blades for use with PSP. The upper diagram shows the distribution of the airfoils and the dimensions of the blades (in inches). The lower diagram shows the rotor instrumentation locations.

four blades, two are pressure instrumented using Kulite pressure sensors. The first instrumented blade has two rows of chord-wise transducers, with rows located at the 93% and 99% radial stations. The second has one chord-wise row at 93% radius. Each row has 10 pressure transducers located on the upper surface, as shown in the lower portion of Figure 3.

The forward flight testing was conducted in the 14x22 facility at NASA Langley Research Center. The tunnel is an atmospheric, closed return tunnel with a test section 14.5 ft (4.4 m) high, 21.75 ft (6.6 m) wide, and 50 ft (15.2 m) long. The tunnel can reach a maximum velocity of 348 ft/s (106 m/s) with a dynamic pressure of 144 psf (6.9 kPa). The achievable Reynolds number of the tunnel ranges from 0 to 2.2 x10^6 per foot (0 to 7.2 x 10^6 per meter). Test section airflow is produced by a 40 ft (12.2 m) 9 bladed fan driven by a 12,000 Hp (8.9 MW) main drive.

The rotor blades were mounted to the General Rotor Model System (GRMS) and a modified ROtor Body INteraction (ROBIN) fuselage. GRMS is a generic rotor drive system that allows testing of different rotor and fuselage configuration. GRMS is powered by two 75 Hp (55.9 kW) water-cooled electric motors that drive a 5.47:1 transmission. Two six component strain gage force and moment balances are contained within GRMS to enable separate measurement of rotor and fuselage loads. The rotor hub is a four bladed fully articulated hub. One blade cuff is instrumented to measure cuff pitch, lead lag, and flapping. Additional instrumentation on GRMS includes an encoder to provide 1/rev and 1024/rev timing signals and accelerometers to monitor machine health. The fuselage is similar to the original ROBIN fuselage with the exception of a rear ramp section. The ROBIN fuselage is an analytically defined representative generic helicopter fuselage that has been used in previous work.[23] The modified ROBIN fuselage used in this test uses the same family of super-ellipse equations as the original ROBIN fuselage while employing a modified set of coefficients to generate the ramp section.

All PSP instrumentation was mounted on the ceiling of the 14x22 so that illumination and image acquisition were performed though Acrylite™ OP-4 windows. OP-4 is a brand of acrylic plastic that can transmit UV light. It also has a high clarity, transmitting ~90% of visible light.

C. Instrumentation

For this test, the light emitting diode (LED) based arrays used in the previous work were exchanged for frequency doubled Nd:YAG lasers (532 nm). A laser-based illumination system was used to attempt to acquire the PSP images needed in one single laser pulse as opposed to several hundred LED flashes (with one flash per revolution). This would provide instantaneous pressure data on the blade while also alleviating issues with the dynamic nature of rotorcraft flight (i.e. blade lead-lag and flap motion). The laser employed was a rugged, compact dual laser head system originally designed for Particle Image Velocimetry (PIV) applications. Because of this, the lasers have been pre-aligned so that the laser path from each head is co-linear and the timing can be manipulated so that both heads fire at the same time. The lasers employed had a nominal power of 150-200 mJ per pulse per head.

An optics stack was designed and built to steer and condition the beam for blade illumination. The optics stack generally consisted of a mirror to steer the beam and a negative lens to expand the beam to a suitable spot size. In addition to the lens, a polycarbonate diffuser was also placed after the lens to remove the fringes caused by the lens and make the illumination spot more uniform. The stack was housed in a holder that allowed for a compact system that could be easily mounted above the windows in the test section ceiling. The typical components of the optics stack are shown in Figure 4a and a completed holder showing the nominal beam path is shown in Figure 4b.

PSP data images were acquired using a specialized interline transfer camera. This was developed specifically for use in PIV applications and operated by masking every other line of the chip, allowing for charge to be transferred quickly (~200 nm transfer time) from the unmasked to the masked region for

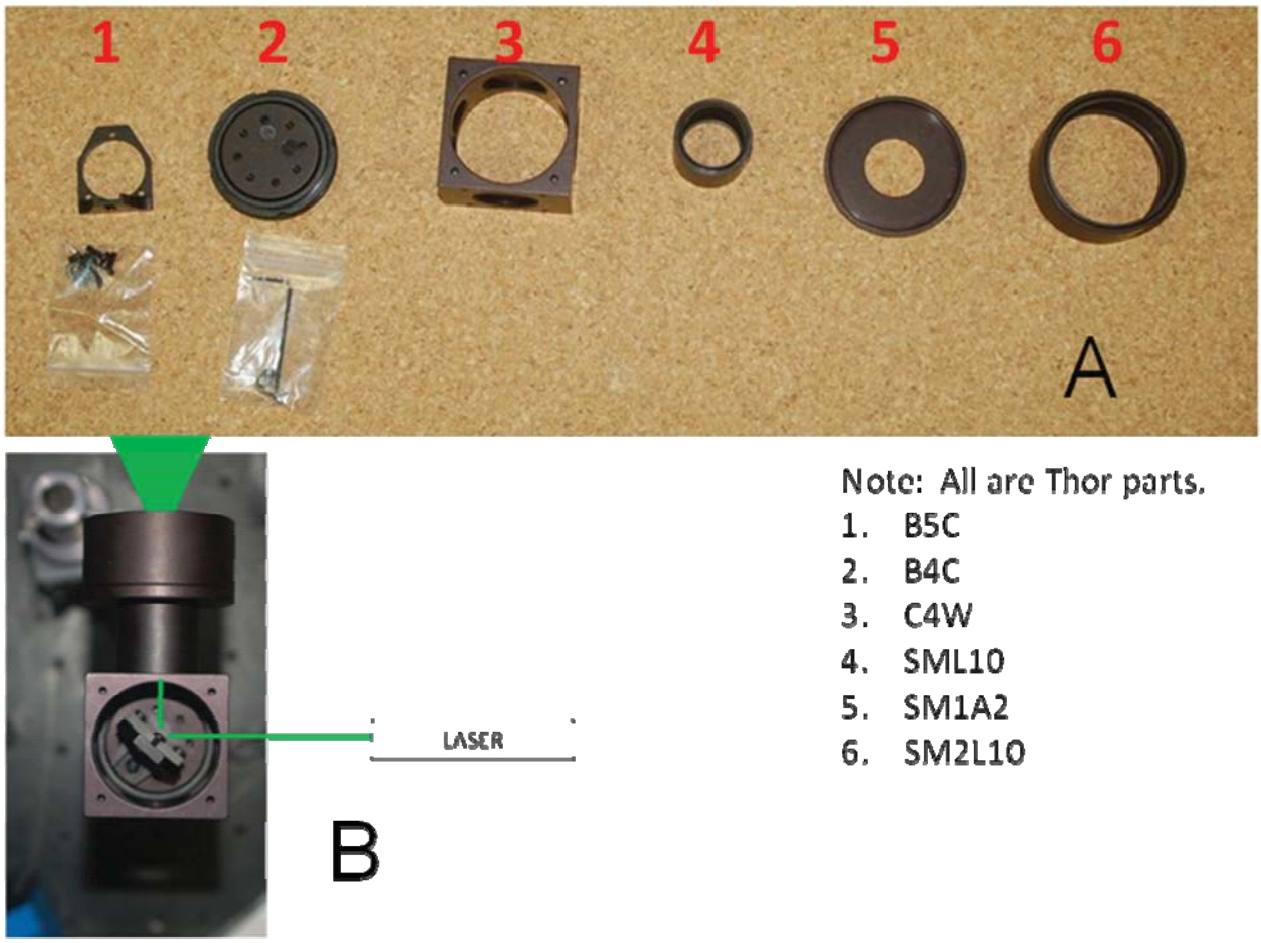

Figure 4. Optics stack components and assembled unit. (A) Individual components and accompanying Thor part numbers. (B) Assembled unit showing optical path.

either storage or readout. This allows for the rapid collection of image pairs with a minimal time delay between images (the interline transfer time above). The camera is also equipped with a fast electronic shutter capable of acquiring an image with an exposure time of as little as 1 μs. The camera employs a CCD chip with an active area of 1600 x 1200 pixels with peak quantum efficiency greater than 50% at 650 nm. The camera has 14-bit digitization as well as on-board memory that will allow it to rapidly store images on the camera, making it possible to run multiple cameras simultaneously from the same computer platform. The camera was binned to 800 x 600 pixels to improve collection efficiency and increase data collection rates.

Due to the testing and safety requirements, it was necessary to have nearly full remote control of pan and tilt as well as focus of the cameras during the test. The cameras were mounted onto a commercial pan/tilt head that was capable of being controlled at distances of several hundred feet. Due to the size of the CCD chip (2/3 inch) and the need for maximum light collection efficiency (or maximum aperture), remote focus and zoom lenses were impractical. Instead, large aperture SLR lenses were used to maximize collection efficiency. Custom designed and built systems were utilized to enable remote focusing during the test. An image showing the camera on the pan/tilt stage as well as with the remote focusing attachment is shown in Figure 5. Full details of the mechanical setup of the camera system will be published at a later date.

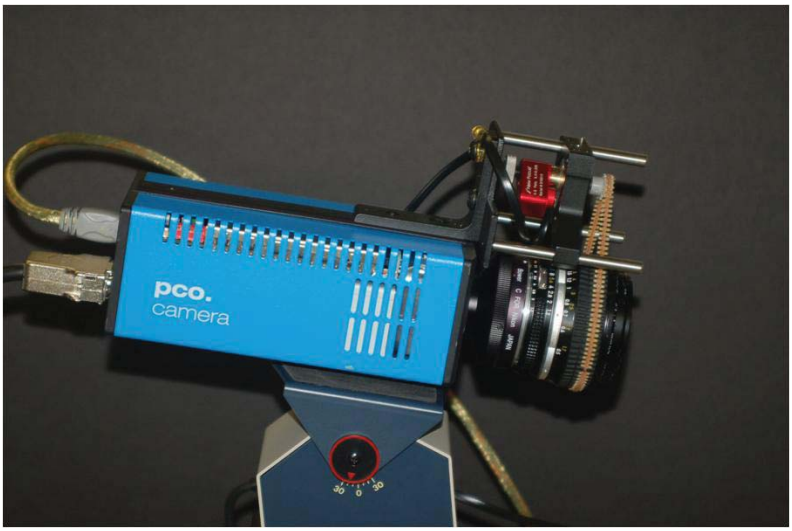

Figure 5. Interline transfer camera affixed to pan/tilt stage and modified with remote focusing device.

D. Data Acquisition

All image acquisition was accomplished using the lifetime-based approach, which was found to be essential in previous test.[16-17] However, these previous tests employed LED-based arrays and functioned by on-chip accumulation of several images to build the necessary data. This was shown to suffer from excessive blurring due to variations in rotational speed, flapping, and lead lag of the blade. Thus, a method to acquire the data in one single rotation was needed to account for this. Using the high powered pulse laser provided sufficient levels of illumination and operating the cameras in the double exposure mode described above allowed the acquisition of the two gate images from one laser pulse. In addition, there was a requirement to synch the actual PSP data acquisition with the wind tunnel dynamic data acquisition system to be able to compare the dynamic pressure transducer measurements with the PSP at the correct azimuthal positions. Timing for the acquisition was accomplished using a custom designed and built system based on a configurable counting board and software interface (Rotor Azimuth Synchronization Program, or RASP) and the signals from the 1/ref and 1024/rev encoders on the GRMS. The RASP allowed for accurate and reproducible alignment of the blades with a specific azimuth location in the rotor disk. Programmable delay generators were also used to synch the camera acquisition with the flashlamp and Q-switch firing of each laser head. The overall control of the data acquisition was accomplished via an external signal sent from the wind tunnel dynamic data acquisition system. Each individual firing of the Q-switch was also recorded by the dynamic data acquisition system to enable comparison between the pressure transducer data with the PSP data at the same rotor azimuth. A simplified diagram of the timing setup is shown in Figure 6.

The actual acquisition of the PSP data was acquired using a double frame imaging technique in which a short exposure image was taken followed immediately by a longer exposure image as detailed by Juliano *et al*.[24] The longer exposure image was started after the interline transfer time of the pixels (200 ns) and lasted as long as it took for the first image to be read into the on-board RAM of the camera. With the arrangement, data could be acquired approximately every 400 ms, and with the current rotor speed, this corresponds to one PSP image pair acquired every 8 revolutions. For an image pair, the camera was set for an initial exposure time of slightly more than 200 μs, corresponding to the optimal delay between flash lamp and Q-switch firing. The initiation of the camera exposure also triggered the programmable delay generator to trigger the flash lamp and Q-switch at the desired times. These times were set to ensure that the laser flash occurred just before the end of the first exposure, exciting the paint. Then the second image was collected so that the remainder of the excited state decay occurred in this frame. A diagram of the nominal PSP imaging process is shown in Figure 7.

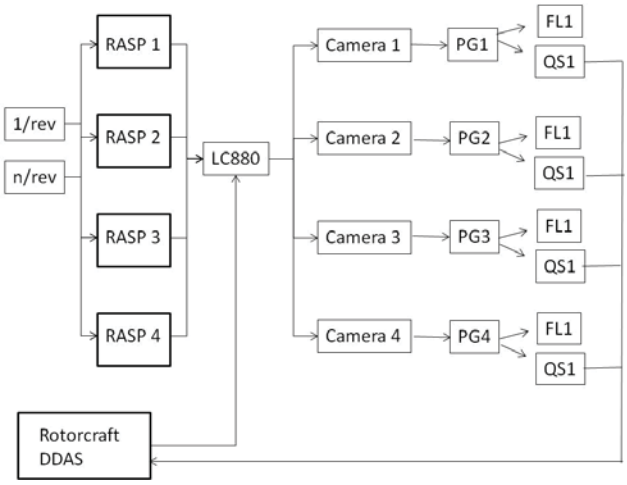

Figure 6. Timing schematic for controlling up to four separate camera/laser systems. PG: Pulse Generator; FL: Flash Lamp; QS: Q-Switch; LC880: Programmable logic gate controller for throttling data acquisition; DDAS: Dynamic Data Acquisition System.

For this test the rotor shaft angle was maintained at -3 degrees and there was no yaw in the model. PSP images were acquired on the Advancing Blade Side (ABS) at an approximate rotor azimuth of 98 degrees and on the Retreating Blade Side (RBS) at an approximate rotor azimuth of 258 degrees. The ABS is the side where the blade is advancing into the freestream velocity and the RBS is the side where the blade is moving in the same direction as the freestream. All data was acquired from the same blade and rotation speed was 1150 rpm.

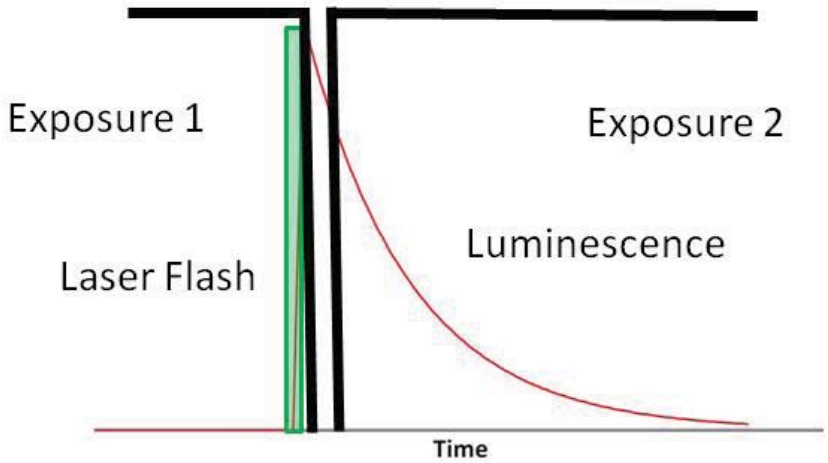

Figure 7. Schematic representation of data acquisition using dual frame imaging and laser pulse excitation. Laser pulse width and delay between images is exaggerated to show difference.

E. Data Analysis

Data analysis for this work followed the standard procedure for analysis of PSP data acquired using the lifetime-based data acquisition procedures with some exceptions. Usually the lifetime-based data analysis is simply dividing Gate 1 by Gate 2 to form an I_{REF}/I image. However, the chosen paint formulation (the porous polymer) displays a significant change in performance that is tied to the application process. This phenomenon has been observed previously in many PSP formulations[25-27] but is very pronounced in this formulation. Essentially, the excited state lifetime of the Pt(TfPP) shows heterogeneity with application, where the lifetime can change dramatically based on the relative localized concentration of the probe. To solve this, a single wind-off image set was acquired immediately after the overspray. Since the overspray was done each morning, this wind-off image set was also acquired each morning. The wind-off image pair served as a further reference for the lifetime data and can account for much of the non-homogeneity effects. The basic data analysis followed the following protocol:

1. Background correction of all images
2. Correlation of wind-on images Gate 1 and Gate 2 to the second gate image of the wind-off pair
3. Creating a "ratio of ratios" image using the wind-off image pair
4. Mapping the resultant image to the surface grid using the previously determined three dimensional coordinates of registration marks added to the blade
5. Final calibration of the image to convert to pressure.

Several of these steps will be explained below.

Correlation of Images and Surface Mapping: For static and quasi-static testing, correlation of the gate images is typically not required when data is acquired in the lifetime mode because both the reference and pressure images are acquired at the same conditions. This usually means that any deformation or model motion that could occur would be minimal. However, in the case of rotor blades, this is not the case. Due to the high degree of aeroelastic bending as well as the dynamic nature of the testing, the two gate images are acquired in one laser pulse. This results in a slight blurring of the second gate image due to the finite excited state lifetime of the luminophore. This blur can be seen in Figure 8, which compares the first gate image (in which the laser pulse fires at the end of the first exposure) with the second gate image (which contains the vast majority of the excited state decay). This blur is caused by both the finite time between the first and second image (~200 ns) as well as the excited state lifetime of the Pt(TfPP) in the binder, which is on the order of 5 μs. The total effect of this is to cause a blur of ~2-3 pixels in the second image. While the actual blurring is not accounted for in this report (please see the Lessons Learned section), it does require a correlation of the image to the reference image for alignment. Furthermore, as a wind-off image pair is used to account for lifetime heterogeneity, a further

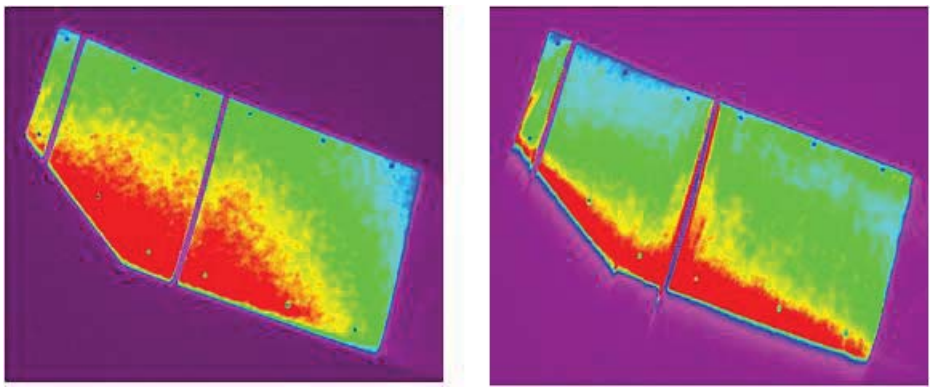

Figure 8. Comparison of first gate (left) and second gate (right) images highlighting the rotational blur that occurs in the second gate (note leading edge).

correlation to these images must also be done.

This correlation was accomplished using registration marks that were placed on the blade using a Sharpee marker. With the registration marks, one can apply an image correlation technique based on a mathematical transformation to empirically map the Gate 2 image to the Gate 1 image, as described in Liu and Sullivan.[9] After the test, the three dimensional locations of the registration marks were measured using the VSTARS technique with respect to the model. With this information it was possible to solve the collinearity equations and transform the image coordinates to physical model coordinates (analogous to model deformation measurements).[9] This allowed the mapping of the PSP image data to a pre-defined surface grid of the blades for later interrogation in software packages such as TecPlot™ as well as easing the direct comparison with computational data.

Ratio and Calibration: After the correlation of the images to the wind-off image pair, the pressure image was calculated by simply ratioing the wind-on images (Gate 1/Gate 2) to form an I_{REF}/I image and then correcting this by dividing the wind-off I_{REF}/I image. Conversion to pressure units was performed using an *a priori* calibration determined above. For this calculation, a temperature on the blade was assumed and then the pressure transducers values were used as a correction factor. This hybrid type of calibration has been described previously.[9]

III. Results and Discussion

A. Improvements from Using Laser-Based Data Acquisition

The benefits from using the laser-based data acquisition technique were apparent from the start. The greatest improvement was the clarity of the images. This is depicted in Figure 9, which shows a comparison of a raw image taken using the LEDs and integrating over multiple revolutions and a raw image from this test. Because of the multiple revolutions that were required for the LED-based approach, the image has noticeable blur around the pressure transducers, especially when compared with the laser-based data acquisition technique. An additional benefit is the greater increase in efficiency. Acquiring a data image over multiple revolutions required data acquisition times on the order a minute to acquire a single image pair. This precluded many of the advantages in signal-to-noise that can be achieved with averaging. Additionally, the comparison with pressure transducers would become tenuous as only an ensemble average could be used over that time frame, severely mitigating any dynamic effects that may exist. Alternatively, with the laser-based data acquisition technique, an image pair can be obtained in single laser flash, corresponding to a single rotation. Now, the comparison with pressure transducers is much cleaner as the image is collected at a single point in time. Additionally, with the current setup, as many as 30 image pairs could be obtained in a single test point collection from the rotorcraft dynamic data acquisition system, which required approximately 15 seconds.

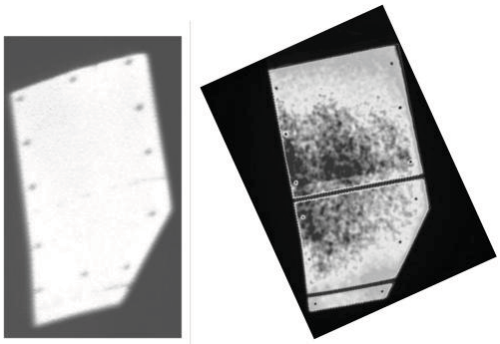

Figure 9. Raw images from LED-based (left) and laser-based (right) data acquisition techniques showing the reduced blurring.

B. Forward Flight Test Results

As mentioned in the Data Analysis section above, a single wind-off image pair was needed to correct some anomalies that happen with this particular paint formulation (the porous polymer PSP). Additionally, there was a contamination element that occurred near the pressure transducers. To protect the pressure transducers from clogging or becoming damaged during the painting process, a thin strip of Kapton tape was placed over the tap rows. While this would necessarily limit some of the data in regions

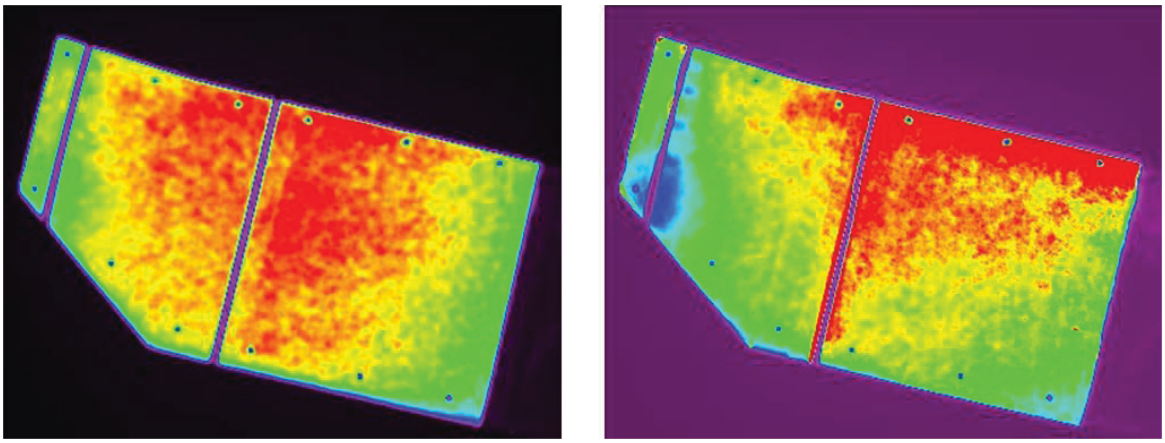

Figure 10. Raw wind-off images. (Left) The First Gate image taken at the laser flash; (B) the second gate image encompassing the majority of the excited-state decay. The contamination from the tape is most noticeable as the blue regions near the 99% chord.

directly at the transducers, another effect was seen. This is shown in Figure 10. In the first gate image (left), the effect is not very noticeable. However, in the second gate image (right) there are significant variations at the tap row at 99% chord. This image contains most of the excited state decay, thus any variations in the lifetime should be convoluted with the actually excitation field. It is currently postulated that this is a contamination from the adhesive of the tape that is dissolved during the overspray process (in which the Pt(TfPP) is applied in a solution of toluene), which may have been applied a bit too heavily at the tip (resulting in a "wetter" overspray). Additionally, the wind-off image pairs were acquired almost immediately after the overspray, so the solvent may not have been allowed to dry sufficiently.

An attempt to mitigate this issue was made by simply "patching" this area of the paint with small regions near the 99% chord row. A comparison of the wind-off I_{REF}/I image before and after the "patching" is shown in Figure 11. Ideally, this image should have a uniform appearance, but lifetime variations in the paint (again, usually caused by application) can be seen. In the unpatched image (left), these variations at the 99% chord are extreme. Patching (right) can remove much of this effect. Obviously this can bias the results in this region, so further study on the effects needs to be carried out as well as strategies to mitigate the effect from happening in the first place. All data analysis was accomplished using the patched reference images.

For the hybrid calibration mentioned in the Data Analysis section, the location of the pressure transducers was virtually moved on the surface grid away from the taped regions. If the pressure

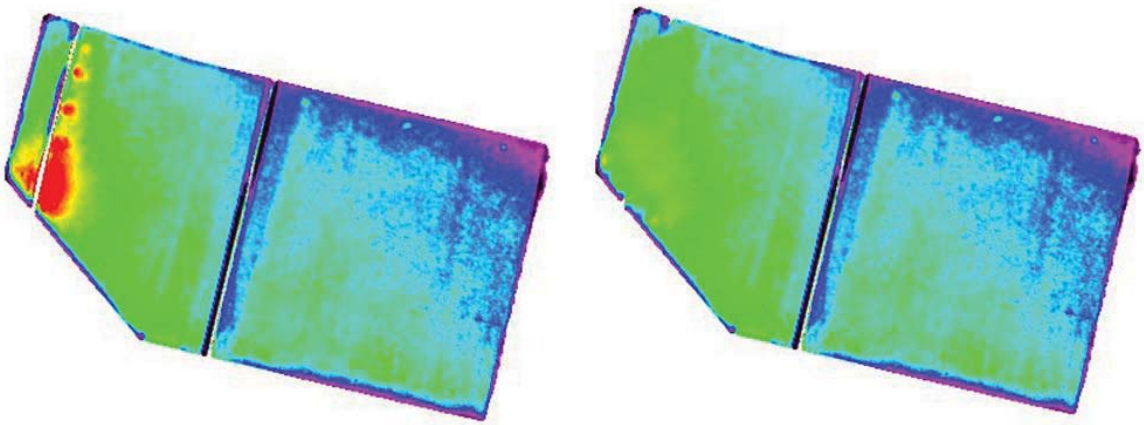

Figure 11. Wind-off I_{REF}/I images. (Left) Unpatched image showing contamination; (right) patched image showing nearly complete removal of the contamination.

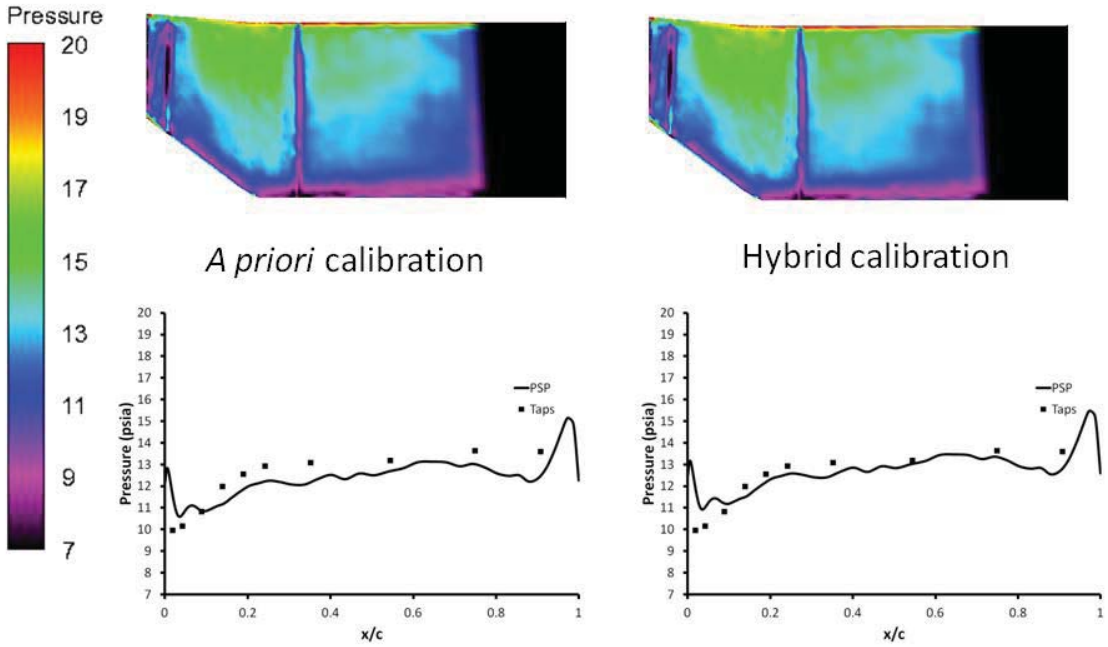

Figure 12. Comparison of PSP data calibrated using the *a priori* calibration (left) and an assumed temperature and the hybrid calibration (right) using the pressure taps to "anchor" the *a priori* calibration. The comparison between the taps and the PSP is shown below each image. The black region on the blade is unmapped data.

transducers would have been covered with only a small piece of tape individually, this probably would not have needed to be done. However, the tape strip afforded the maximum protection to the transducers, as well as significantly reduced the amount of time needed for application. For the final data analysis, the transducers were moved toward the hub about 0.3 inches (the original location was on a station at 108.6" and they moved to 108.3"). This move was also structured to maintain the same locations in x/c as were in the original. This moved the transducers a significant (> 5 pixels) distance from the tap to allow their use in calibration (the spatial resolution in the blade is ~0.03"/pixel) while keeping a close proximity to their actual location.

With the transducers virtually moved to a clear region, they can now be used to anchor the *a priori* calibration, which was calculated using an assumed temperature. A comparison of the *a priori* calibration with the hybrid calibration is shown in Figure 12. The comparison between the pressure tap measurements and the PSP data is also included and shows that the hybrid calibration does bring the PSP data closer in line to the transducers. It should also be noted that the PSP data at the extremely low and high x/c locations is probably biased due to blurring in the second gate (as mentioned above). Even with this, the PSP shows relatively good agreement with the transducers. For consistency, all final calibrations were done using the hybrid calibration technique to anchor the *a priori* calibration.

The first set of runs was acquired at a constant velocity of 138 knots (71.0 m/s) and at four thrust coefficients. A comparison of a PSP image at each thrust condition is shown in Figure 13. This is the ABS and shows good qualitative agreement with what should be expected. It also shows that the pressure on the blade at this position has little dependence on the thrust coefficient. The comparison between the pressure transducers and the PSP is also shown in Figure 14, and shows the same result. The PSP does not agree as well as the previous figure, most likely due to the smaller pressure changes on the model as well as not accounting for the blur. However, both the PSP and the transducers show the higher pressure region at the extreme leading edge with the pressure decreasing as the flow accelerates over the center of the blade, flowed by a gradual return to higher pressure at the trailing edge. As with the PSP data, the pressure tap measurements also show little dependence on the thrust coefficient.

However, the same cannot be said of the blade in the "retreating" position (the blade is moving with the air flow in the tunnel). Figure 15 shows PSP data taken from the same blade during the same rotation, but retreating from the air flow. The PSP data shows that there is a much larger dependence on the thrust coefficient, as evidenced by the lower pressure region near the leading edge of the blade. Additionally, there is evidence of a flow phenomenon near the blade tip, such as a vortex shedding off the tip. This is highly dependent on the thrust coefficient, and evidence of it can be seen from C_T greater than 0.006. The larger pressure differentials are also evident from the pressure tap and PSP comparisons, which is shown in Figure 16. As with the previous data, the tap agreement is very good (except near the leading and trailing edge). However, the flow phenomenon that is seen in the PSP at the tip does not appear in the tap data. From visual inspection of the PSP data, it seems that the phenomenon flows just past the last pressure tap, or possibly between two transducers. This does show one of the greatest advantages to using PSP: the ability to visualize and measure global pressure distributions as opposed to localized pressure measurements as is acquired from pressure transducers.

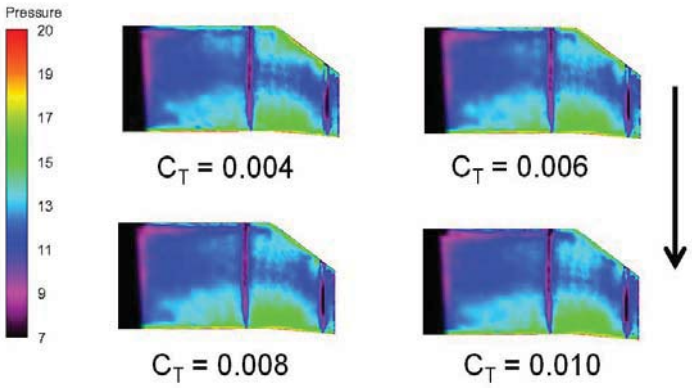

Figure 13. PSP images acquired from the ABS. The arrow represents the direction of the tunnel flow. The black regions on the blade are unmapped data.

A test condition was also run to maximize the suction peak on the blades by increasing the thrust coefficient to $C_T = 0.012$. In addition the forward speed was reduced to 120 knots (61.7 m/s). the results from both the advancing and retreating position of the blade as well as the pressure tap comparisons are

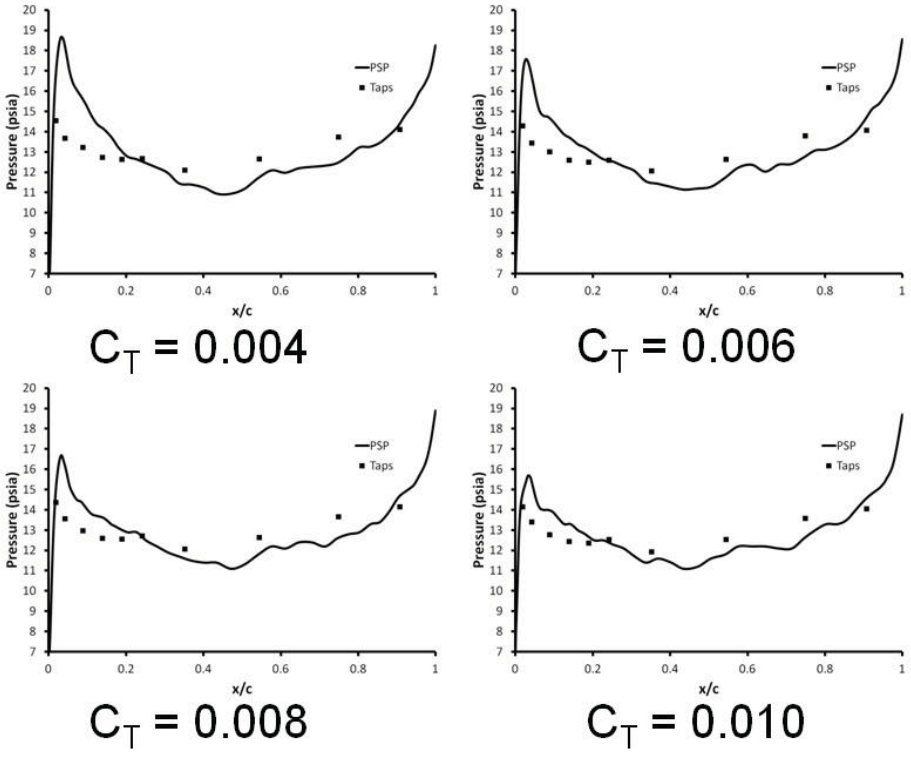

Figure 14. ABS comparisons between PSP data and pressure tap measurements from Figure 13.

shown in Figure 17. As was the case in the previous testing, the advancing blade position shows little dependence on the thrust coefficient. The retreating blade position shows much the same behavior as well, though the overall pressure at the leading edge is lower due to increased thrust coefficient. However, the flow phenomenon at the tip is much more pronounced at this condition with possibly some flow structure inside observable.

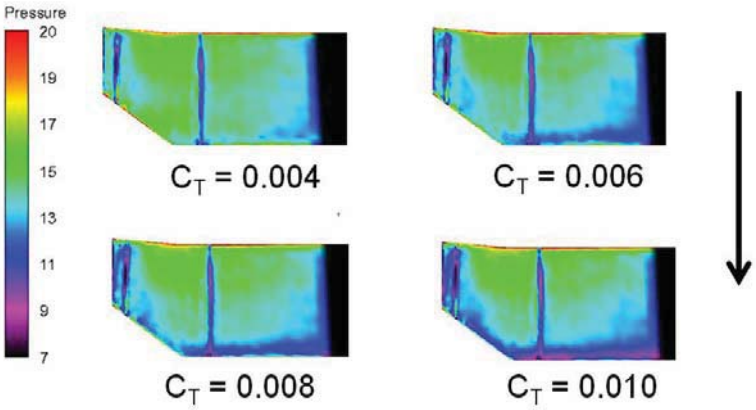

Figure 15. PSP images acquired from the RBS. The arrow represents the direction of the tunnel flow. The black regions on the blade are unmapped data.

Finally, because of the large increase in data collection efficiency of the laser-based data acquisition technique, it is now possible to visualize and measure the variation in pressure on the blade during each rotation. This is illustrated in Figure 18 in which three individual sets of data from one data point are interrogated. This is the same condition from Figure 17 and only the retreating blade position is considered. These data were taken approximately 80 revolutions apart and represent approximately 66% of the time used to collect a data point by the dynamic data acquisition system. From the images, it is readily apparent that there is variation across the blade, especially in the magnitude of the pressure. This is borne out in comparison between the three images. In this comparison, only the PSP data is considered and shows a variation of about 1 psi through the center of the blade. Once the rotational blur is accounted for, analysis of the edges can also be carried out. Additionally, the flow phenomenon that occurs at the tip does seem dynamic in nature as it is visible changing throughout the run.

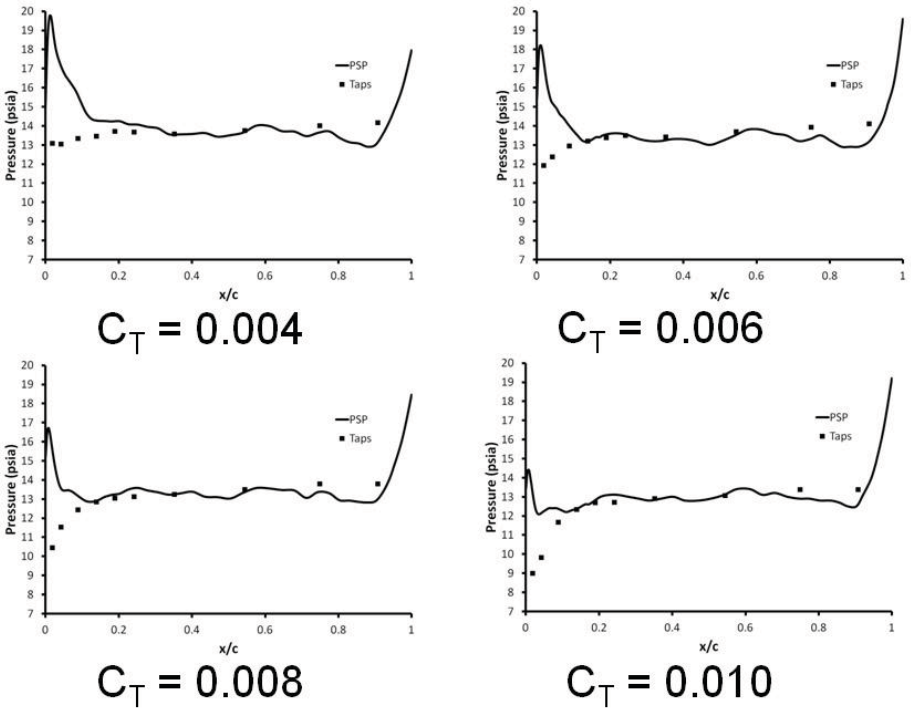

Figure 16. RBS comparisons between PSP data and pressure tap measurements from Figure 15.

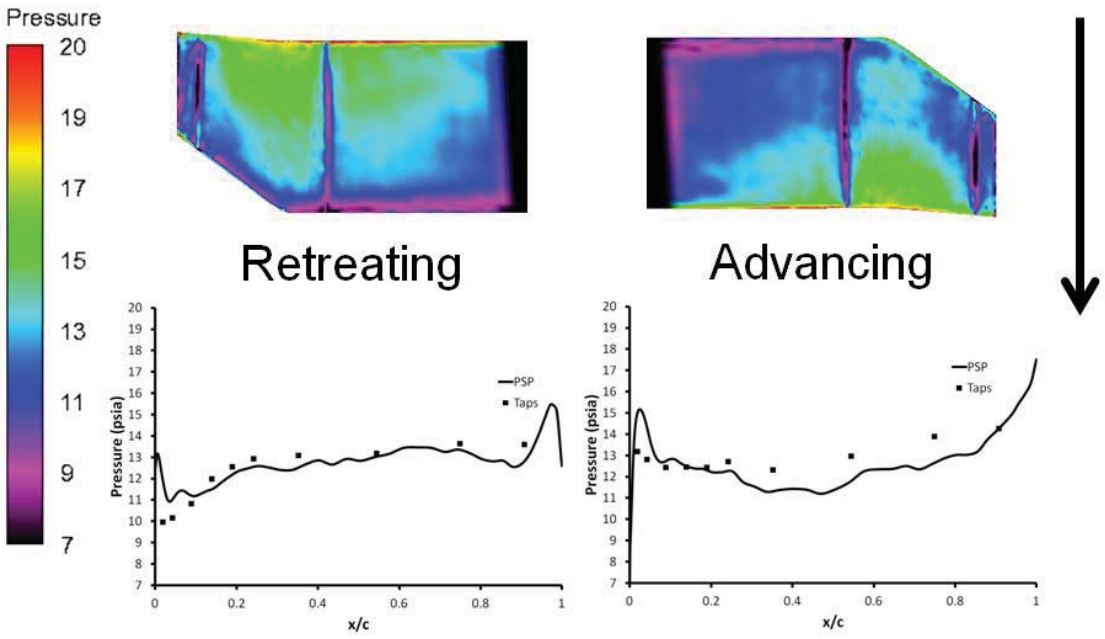

Figure 17. PSP images and pressure tap comparison from the advancing and retreating blade position at a $C_T = 0.012$. The arrow represents the direction of the tunnel flow. The black regions on the blade are unmapped data.

IV. Lessons Learned/Future Directions

This section will detail several of the lessons learned in this test as well as possible solutions to these challenges. It is anticipated that another test will be forthcoming in FY12 and further development of the technique will find much interest in current rotorcraft designers. The major challenges stem from the paint and its application and accounting for the rotational blur that is inherent in this technique.

A. Paint

The porous polymer employed in this test is a vast improvement over the sol-gel-based formulation used in the previous testing.[16-17] However, there are still some limitations of this paint, most notably in the application and the temperature sensitivity. The ceramic compound that is the major component of the binder is very abrasive, thus requiring the protection of the pressure transducers. In conventional testing using static pressure transducers, this can be easily accomplished by simply purging the pressure tap orifices using compressed shop air. This has been used historically and has always shown good results. However, this test required the use of dynamic pressure transducers. These transducers are essentially thin diaphragms that need to be mounted on or very near the surface. As a consequence, the typical purging methods are no longer applicable, nor are methods such as blocking the orifices with wire. For this test, the only solution was to use a strip of Kapton tape. While this protected the transducers (as evidenced by their continued functionality), two issues were introduced that needed to be overcome. First, there was no PSP data directly at the pressure transducers. This could be mitigated by simply adjusting the virtual positions of the transducers on the surface grid. While not ideal, this is a valid procedure if the area in question is large enough and there are no discrete surface events occurring (like shocks or vortices).

The bigger issue that occurred was the contamination that was evident near the taped region. While there is more laboratory work to be done on this, it appears that this is most likely a result of the overspray process itself. The solvent used in the overspray could be dissolving some of the adhesive that

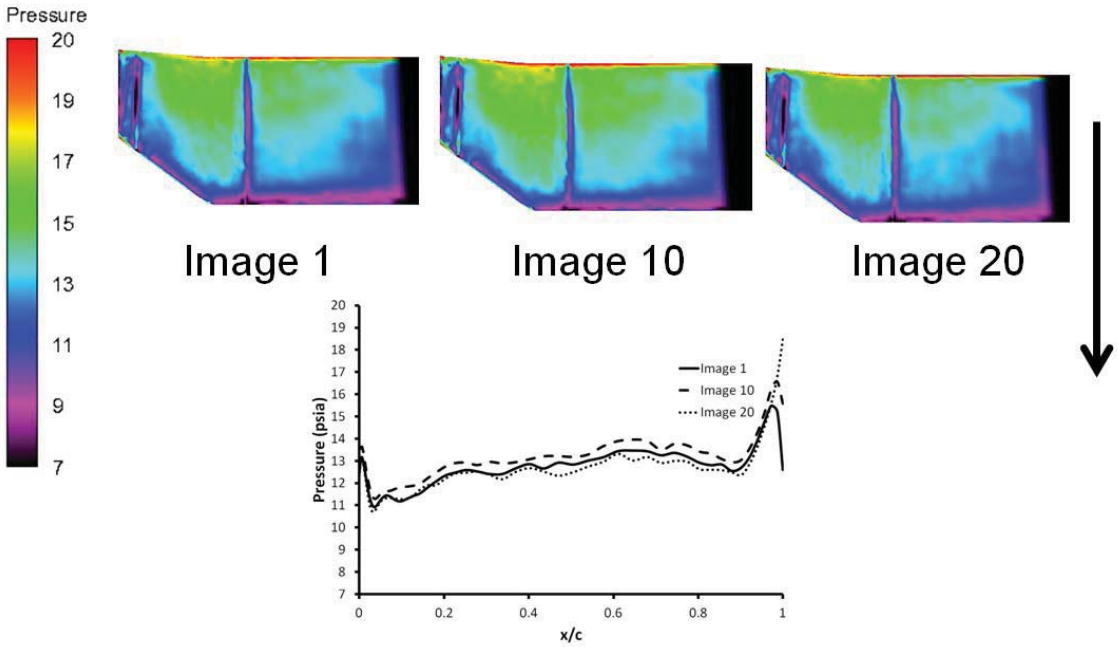

Figure 18. Three separate PSP images acquired at the same conditions as Figure 17. These images were acquired approximately 80 revolutions apart. The arrow represents the direction of the tunnel flow. The black regions on the blade are unmapped data.

is in turn flowing into the binder causing a change in the local environment of the luminophore. This leads to lifetime heterogeneity in the paint that needs to be addressed. Since it appears to manifest itself most in the wind-off image, this portion was patched to remove the contamination. This is definitely not an ideal solution and laboratory work to identify the cause and how to mitigate this are currently underway.

Finally, the temperature sensitivity of the porous polymer paint is one of its main limitations. As can be seen in Figure 2, there is a large spread in the sensitivity curves due to temperature. While this conceivably could be accounted for in processing, this would require a pixel-by-pixel knowledge of the temperature to do it most accurately. In this case, assuming a single temperature seems to work (at least close to the transducers), but this will not always be the case. This temperature sensitivity is mostly due to the binder itself and how the diffusion of oxygen into (and out of) the binder is affected by temperatures. Even in an ideal paint, there will be a temperature dependence due to the physical nature of luminescence. However, that dependence is up to an order of magnitude smaller than the binder effect. The temperature sensitivity issue with PSP formulations has been an ongoing development area and to date, there are few formulations that can approach the limit of temperature sensitivity. One of these formulations has also been modified to exhibit a high frequency response. Though not as high as the porous polymer, it should be sufficient for most rotorcraft applications. This binder is based on a fluoro-isopropyl-butyl (FIB) copolymer. A sample calibration curve compared to the porous polymer formulation is shown in Figure 19, showing that the FIB formulation (circles) has a much narrower distribution than the porous polymer (squares). Further investigation of this formulation for dynamic PSP applications is currently under study.

B. Rotational Blur

Owing to the finite excited-state lifetime and the inherent time between exposures, the second gate typically exhibited a blur of 2-3 pixels in the image as shown previously in Figure 8. This blur is especially evident at the leading edge. To account for this, several algorithms are currently under development and are being tested. These are based on a variety of deconvolution algorithms. Once tested, these data will be reanalyzed to see the effects, especially near the leading and trailing edge. This

should enable a better visualization of these areas where larger pressure gradients are expected to be seen. This will also greatly decrease the discrepancies between the PSP and the pressure transducers in these regions as seen in Figures 14 and 16.

V. Conclusions

This report details a test of using PSP for the global pressure determination on the tips of rotorcraft blades in forward flight. This test was performed using the General Rotor Model System installed in the 14- x 22-Foot Subsonic Tunnel at NASA Langley Research Center. Two rotor blades were painted with a porous polymer PSP formulation capable of frequency responses on the order of 20 kHz. The blades were instrumented with pressure transducers, with the actual blade used in the measurement instrumented with a row at 93% and 99% chord, respectively (though only the 99% chord was functional). The blades were tested at various forward velocities and thrust coefficients.

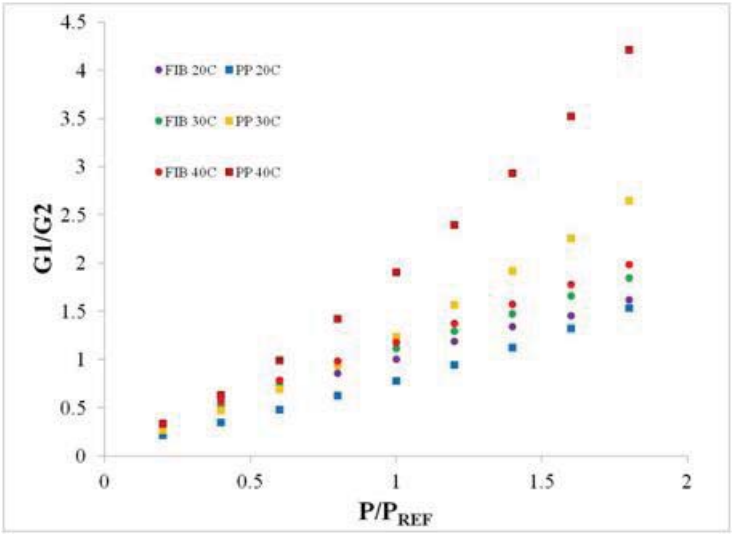

Figure 19. Representative calibration comparison between a FIB binder (circles) and a porous polymer binder (squares) highlighting the lower temperature sensitivity of FIB. Courtesy of Innovative Scientific Solutions, Inc.

For this test, a laser-based data acquisition system was designed and deployed. This system was capable of measuring a single blade through up to four different positions in the rotor disk thorough a single revolution. This was accomplished by exciting the paint with the laser and using an interline transfer camera to take a pair of images. With correct timing, the laser flash occurs at the end of the first gate with the majority of the excited-state decay being recorded by the second gate. This is analogous to the traditional lifetime-based approach in which two images are collected, one during the excitation pulse, and one after the pulse. However, with the power of the laser, all data could be acquired in one rotation with one laser pulse. Thus, data collection is inherently more efficient as well as the possibility of recording dynamic pressure data is a possibility.

Analysis of the data shows fairly good agreement (within 10%) of the pressure tap measurements, though there are some issues that were encountered. To protect the pressure transducers, Kapton tape was placed over the transducers. During the application of the PSP, the solvent seems to have caused some of the adhesive to dissolve and leach into the binder, leading to some significant effects in this region. This was patched with nearby data to mitigate the results. Additionally, the temperature sensitivity of the PSP is a limiting factor in the accuracy of the data, though this can be lessened using the pressure tap reading to correct the bias. Finally, there was no attempt to account for the rotational blur seen in these data, resulting is suspect results near the leading and trailing edge.

Even with these limitations, the data agreed both qualitatively and somewhat quantitatively with the expected results. In addition, there is evidence of a vortex shedding or other flow phenomenon that can be seen dependent on both blade position (retreating or advancing) and thrust coefficient. To date, this is one of the first successful tests of PSP on flexible rotating surfaces capable of measuring dynamic phenomena.

Finally, several methods to further improve the measurement technique have been discussed. These include optimizing paint application strategies as well as employing a different formulation that exhibits

much lower temperature sensitivity. Additionally, algorithms to account for the rotational blur in the images while maintaining data integrity are also under development and will be tested in the near future.

References

1. Lorber, P.F., Stauter, R.C., and Landgrebe, A.J., "A Comprehensive Hover Test of the Airloads and Airflow of an Extensively Instrumented Model Helicopter Rotor," *Proceedings of the 45th Annual Forum of the American Helicopter Society*, Boston, MA, May 1989.

2. Lal, M.K., Liou, S.G., Pierce, G.A., and Komerath, N.M., "Measurements around a Rotor Blade Excited in Pitch, Part 2: Unsteady Surface Pressure," *Journal of the American Helicopter Society*, Vol. 39, No. 2, 1994, pp. 13-20.

3. Gorton, S.A., Poling, D.R., and Dadone, L., :Laser Velocimetry and Blade Pressure Measurements of a Blade-Vortex Interaction," *Journal of the American Helicopter Society*, Vol. 40, No. 2, 1995, pp. 15-23.

4. Lorber, P.F., "Aerodynamic Results of a Pressure-Instrumented Model Rotor Test at the DNW," *Proceedings of the 46th Annual Forum of the American Helicopter Society*, Washington, DC, May 1990.

5. Kavandi, J., Callis, J., Gouterman, M., Khalil, G., Wright, D., Green, E., Burns, D., and McLachlan, B., "Luminescent Barometry in Wind Tunnels," *Review of Scientific Instrumentation*, Vol. 61, No. 11, 1990, pp. 3340-3347.

6. Morris, M.J., Benne, M.E., Crites, R.C., and Donovan, J.F., "Aerodynamic Measurements Based on Photoluminescence," *31st Aerospace Sciences Meeting*, AIAA, Reno, NV, 1993, Paper 93-0175.

7. McLachlan, B., and Bell, J., "Pressure-Sensitive Paint in Aerodynamic Testing," *Experimental Thermal and Fluid Science*, Vol. 10, No. 4, 1995, pp. 470-485.

8. Liu. T., Campbell, B., Burns, S., and Sullivan, J., "Temperature- and Pressure-Sensitive Luminescent Paints in Aerodynamics," *Applied Mechanics Reviews*, Vol. 50, No. 4, 1997, pp. 227-246.

9. Liu, T., and Sullivan, J., *Pressure and Temperature Sensitive Paints (Experimental Fluid Dynamics)*, Springer-Verlag, Berlin, 2004.

10. Lakowicz, J., *Principles of Fluorescence Spectroscopy*, 2nd ed., Kluwer Academic/Plenum Publishers, New York, 1999, pp. 239-242.

11. Engler, R., and Klein, C., "DLR PSP System: Intensity and Lifetime Measurements," *17th International Congress on Instrumentation in Aerospace Simulation Facilities*, IEEE, Pacific Grove, CA, 1997, pp. 46-56.

12. Holmes, J., "Analysis of Radiometric, Lifetime, and Fluorescent Imaging for Pressure Sensitive Paint," *Aeronautical Journal*, Vol. 102, No. 1014, 1998, pp. 189-194.

13. Bell, J.H., Schairer, T.E., Hand, L.A., and Mehta, R.D., "Surface Pressure Measurements Using Luminescent Coatings," *Annual Review of Fluid Mechanics*, Vol. 33, 2001, pp. 115-206.

14. Mitsuo, K., Egami, Y., Asai, K., Suzuki, H., and Mizushima, H., "Development of Lifetime Imaging System for Pressure-Sensitive Paint," *22nd AIAA Aerodynamic Measurement Technology and Ground Testing Conference*, AIAA, St. Louis, MO, 2002, Paper 2002-2909.

15. Watkins, A.N., Jordan, J.D., Leighty, B.D., Ingram, J.L., and Oglesby, D.M., "Development of Next Generation Lifetime PSP Imaging Systems," *20th International Congress on Instrumentation in Aerospace Simulation Facilities*, IEEE, Gottingen, Germany, 2003, pp. 372-382.

16. Wong, O.D, Watkins, A.N., and Ingram. J.L., "Pressure Sensitive Paint Measurements on 15% Scale Rotor Blades in Hover," *35th AIAA Fluid Dynamics Conference*, AIAA, Ontario, Canada, 2005, Paper 2005-5008.

17. Watkins, A.N., Leighty, B.D., Lipford, W.E., Wong, O.D., Oglesby, D.M., and Ingram. J.L., "Development of a Pressure Sensitive Paint System for Measuring Global Surface Pressures on Rotorcraft Blades," 22nd *International Congress on Instrumentation in Aerospace Simulation Facilities*, IEEE, Pacific Grove, CA, 2007, and published in the proceedings.

18. Scroggin, A.M., Slamovich, E.B., Crafton, J.W., Lachendro, N., and Sullivan, J.P., "Porous Polymer/Ceramic Composites for Luminescence-Based Temperature and Pressure Measurement," *Materials Research Society Symposium Proceedings*, Vol. 560, pp. 357-352.

19. Scroggin, A.M., *Processing and Optimization of Doped Polymer/Ceramic Composite Films for Luminescence-Based Pressure and Temperature Measurement in Aerodynamic Applications,* MS Thesis, School of Material Science and Engineering, Purdue University, 1999.

20. Gregory, J.W., Asai, K., Kameda, M., Liu, T., and Sullivan, J.P., "A Review of Pressure-Sensitive Paint for High-Speed and Unsteady Aerodynamics," *Proceedings of the Institution of Mechanical Engineers – Part G: Journal of Aerospace Engineering*, Vol. 222, No. 2, pp. 249-290.

21. Noonan, K.W., "Aerodynamic Characteristics of Two Rotorcraft Airfoils Designed for Application to the Inboard Region of a Main Rotor Blade," NASA-TP-3009, AVSCOM-TR-90-B-005, 1990.

22. Noonan, K.W., "Aerodynamic Characteristics of Two Rotorcraft Airfoils Designed for the Tip Region of a Main Rotor Blade," NASA-TM-4264, AVSCOM-TR-91-B-003, 1991.

23. Wong, O.D. and Watkins, A.N., "Blade Tip Pressure Measurements Using Pressure Sensitive Paint," to be presented at the *AHS International 68th Annual Forum*, AHS, Fort Worth , TX, 2011.

24. Juliano, T.J., Kumar, P., Peng, D., Gregory, J.W., Crafton, J., and Fonov, S., "Single-Shot, Lifetime-Based Pressure-Sensitive Paint for Rotating Blades," *Measurement Science and Technology*, Vol. 22, No. 8, 2011, 085403 (10pp).

25. Bell, J.H., "Accuracy Limitations of Lifetime-Based Pressure-Sensitive Paint (PSP) Measurements," *19th International Congress on Instrumentation in Aerospace Simulation Facilities*, IEEE, Cleveland, OH, 2001, pp. 5-16.

26. Ruyten, W. and Sellers, M., "Lifetime Analysis of the Pressure-Sensitive Paint PtTFPP in FIB," *42nd Aerospace Sciences Meeting*, AIAA, Reno, NV, 2004, Paper 2004-881.

27. Ruyten, W., Sellers, M.E., and Baker, W.M., "Spatially Nonuniform Self-Quenching of the Pressure-Sensitive Paint PtTFPP/FIB," *47th Aerospace Sciences Meeting*, AIAA, Orlando, FL, 2009, Paper 2009-1660.

REPORT DOCUMENTATION PAGE

Form Approved
OMB No. 0704-0188

1. REPORT DATE *(DD-MM-YYYY)*	2. REPORT TYPE	3. DATES COVERED *(From - To)*
01- 12 - 2011	Technical Memorandum	

4. TITLE AND SUBTITLE

Deployment of a Pressure Sensitive Paint System for Measuring Global Surface Pressures on Rotorcraft Blades in Simulated Forward Flight - Preliminary PSP Results From Test 581 in the 14- x 22-Foot Subsonic Tunnel

5a. CONTRACT NUMBER

5b. GRANT NUMBER

5c. PROGRAM ELEMENT NUMBER

6. AUTHOR(S)

Watkins, Anthony N.; Leighty, Bradley D.; Lipford, William E.; Wong, Oliver D.; Goodman, Kyle Z.; Crafton, James; Forlines, Alan; Goss, Larry P.; Gregory, James; Juliano, Thomas J.

5d. PROJECT NUMBER

5e. TASK NUMBER

5f. WORK UNIT NUMBER

877868.02.07.07.06.03.01

7. PERFORMING ORGANIZATION NAME(S) AND ADDRESS(ES)

NASA Langley Research Center
Hampton, VA 23681-2199

8. PERFORMING ORGANIZATION REPORT NUMBER

L-20095

9. SPONSORING/MONITORING AGENCY NAME(S) AND ADDRESS(ES)

National Aeronautics and Space Administration
Washington, DC 20546-0001

10. SPONSOR/MONITOR'S ACRONYM(S)

NASA

11. SPONSOR/MONITOR'S REPORT NUMBER(S)

NASA/TM-2011-217316

12. DISTRIBUTION/AVAILABILITY STATEMENT

Unclassified - Unlimited
Subject Category 35
Availability: NASA CASI (443) 757-5802

13. SUPPLEMENTARY NOTES

14. ABSTRACT

This report will present details of a Pressure Sensitive Paint (PSP) system for measuring global surface pressures on the tips of rotorcraft blades in simulated forward flight at the 14- x 22-Foot Subsonic Tunnel. The system was designed to use a pulsed laser as an excitation source and PSP data was collected using the lifetime-based approach. With the higher intensity of the laser, this allowed PSP images to be acquired during a single laser pulse, resulting in the collection of crisp images that can be used to determine blade pressure at a specific instant in time. This is extremely important in rotorcraft applications as the blades experience dramatically different flow fields depending on their position in the rotor disk. Testing of the system was performed using the U.S. Army General Rotor Model System equipped with four identical blades. Two of the blades were instrumented with pressure transducers to allow for comparison of the results obtained from the PSP. This report will also detail possible improvements to the system.

15. SUBJECT TERMS

Dynamic pressure measurements; Non-intrusive measurements; Optical diagnostics; Pressure Sensitive Paint

16. SECURITY CLASSIFICATION OF:			17. LIMITATION OF ABSTRACT	18. NUMBER OF PAGES	19a. NAME OF RESPONSIBLE PERSON
a. REPORT	b. ABSTRACT	c. THIS PAGE			STI Help Desk (email: help@sti.nasa.gov)
					19b. TELEPHONE NUMBER *(Include area code)*
U	U	U	UU	23	(443) 757-5802